MECHANICAL PROPERTIES OF CARBON-BASED NANOCOMPOSITES FOR SENSORS USED IN BIOMEDICAL APPLICATIONS

Maria Roxana MARINESCU[1], Bogdan Cătălin ȘERBAN[2], Cornel COBIANU[3], Niculae DUMBRĂVESCU[4], Octavian IONESCU[5], Octavian BUIU[6], Liviu Daniel GHICULESCU[7]

In this paper, we present our initial findings related to the response of carbon nanohorns nanocomposites, processed as films with polyvinylpyrrolidone as matrix. Films having 1-8 sensitive layers (denoted 1L, 2L, 3L, 4L, 5L, 6L, 7L and 8L) of composite were subjected to mechanical stress and various temperature changes. A quick mechanical stress test was made by applying different loads (2 N, 5 N, 10 N and 20 N). We obtained Young elasticity modulus of 8.33 MPa (1L) and 3.99 MPa (8L). The electrical resistances of the sensors were measured for each deposition, showing a decrease from 838 Ω to 562 Ω (from 1L to 8L deposited). Optical microscopy images showed that the solution used as sensitive layer is resistant to temperatures from +50 ^{0}C to -50 ^{0}C.

Keywords: Oxidized carbon nanohorns, PVP-carbon nanohorns composite films, static mechanical load vs. deformation, deformation vs. film thickness, behavior at thermal cycling

1. Introduction

The medical field (including here all the aspects – prevention, monitoring, clinical intervention, physical and physiological rehabilitation) was and still is one of the driving forces for the development of new, more performant instruments

[1] PhD student at University POLITEHNICA of Bucharest; IDT, National Institute for Research and Development in Microtechnologies, IMT-Bucharest, Voluntari, Romania, e-mail: roxana.marinescu@imt.ro

[2] CS III, National Institute for Research and Development in Microtechnologies, IMT-Bucharest, Voluntari, Romania, e-mail: bogdan.serban@imt.ro

[3] CS I, National Institute for Research and Development in Microtechnologies, IMT-Bucharest, Voluntari, Romania e-mail: cornel.cobianu@imt.ro

[4] CS III, National Institute for Research and Development in Microtechnologies, IMT-Bucharest, Voluntari, Romania e-mail: niculae.dumbravescu@imt.ro

[5] CS III, National Institute for Research and Development in Microtechnologies, IMT-Bucharest, Voluntari, Romania e-mail: octavian.ionescu@imt.ro

[6] CS III, National Institute for Research and Development in Microtechnologies, IMT-Bucharest, Voluntari, Romania e-mail: octavian.buiu@imt.ro

[7] Prof., Dept. of Machine Building Technology, University POLITEHNICA of Bucharest, Romania, e-mail: daniel.ghiculescu@upb.ro

and operating devices, adapted to the specific requirements of the field: reliability, biomedical compatibility, and ease of use. In particular, the recent advancements in the use of wearable devices for monitoring the patient's health status brought into discussion the need for precise regulatory requirements to support the faster deployment of the devices from design, laboratory tests, towards real-life clinical trials and, finally, on the market [1].

Carbon-based nanomaterials (CBNs) and their nanocomposites have been – over more than a decade – in the limelight of the scientific and industrial communities. The CBN's - graphene (and its derivatives, such as graphene oxide - GO, reduced graphene oxide - rGO, graphene quantum dots – GQDs, carbon nanotubes - CNTs, carbon nanohorns - CNHs, nanocrystalline graphene - NCG, etc.) have become especially important over the past years due to their unique chemical, electrical or mechanical properties. They have shown, overall promising results for a wide range of applications: biomedicine (targeted drug delivery, bio-sensing, or cell imaging [2], regenerative [3], and therapeutical medicine [4], nanosystems for breast cancer detection and treatment [5]); industrial [6, 7]; green energy generation and storage [8, 9]; gas sensing [10-12].

The CBN's used in living systems have opened the way for the investigation of their potential applications in an emerging field of nanomedicine [13]. Each member of the carbon family exhibits specific and, up to a point unique features; all these have been exploited in diverse biological applications including biosensing, tissue engineering, diagnosis, drug delivery, imaging, and cancer therapy [14]. Santos et al. [15] focused on amorphous carbon films – with high potential as a biomaterial used during cardiovascular surgeries. Another great example is presented by Xie et al. [16], where a graphene-based supercapacitor is used as a flexible wearable sensor for monitoring pulse-beat. The invention focused on the advantages of the graphene, which is thin, extremely sensitive, and highly adaptable.

Carbon nanostructures (CBNs) can play a significant role in the multidisciplinary approach needed in the development of neuro-regenerative techniques, where neuroregeneration is the regrowth, restoration, or repair of degenerated nerves and nervous tissues [17]. Carbon nanotubes (CNTs), in particular, have shown to interact with the nervous system promoting neural development; moreover, artificial nerve conduits were built of absorbable synthetic materials [18]. Studying the properties of CBNs, it can be seen that they are very suitable for bio-sensing [19]. Many humidity sensors are used in biomedical applications; one such example is described in [20], where a wearable humidity sensor - used to sense and record relative humidity levels (RH) in nasal and oral breath - is presented. The sensor has high sensitivity and rapid time of response. The idea of using humidity sensors for measuring the sweat rate was discussed by Salvo et al. in [21], where such sensors have been embedded into

textile substrates, and their functionality – continuous monitoring of the sweat levels - demonstrated. Sweat - composed 99% from water - is a promising biofluid used in clinical analysis having the great advantage of its non-invasive sampling [22]. Evaporation of sweat from skin surfaces effectively dissipates heat generated by a hot environment or physical activity. Calcium is crucial to driving sweating [23]. Other essential data can be extracted from the sweat levels: the most concentrated solute in sweat is NaCl; the rate of sweating can lead us to different problems of the human body [24].

On the other hand, single-walled carbon nanohorns (SWCNHs), a kind of 0D carbon - nanoallotrop consisting of horn-shaped sheath aggregate of graphene sheets, were first reported by Iijima in 1999 [25]. These carbon nanostructures exhibit outstanding properties such as high dispersibility, large specific surface area, excellent thermal, electrical, and mechanical properties, versatile synthesis procedure, availability for covalent and noncovalent functionalization [26]. Due to their specific spherical shape of sub-micron diameter carbon nanohorns are expected to have attractive tribological and thermal properties. Miyawaki et al. [27] and Fan et al. [28] made some investigations on thermal treatment of the nanohorns at high temperature (~1500 K). The results showed that the formation of junction structures, based on well-reorganized carbon networks, was significantly enhanced. They investigated the coalescence and melting behaviors of carbon nanohorns at temperatures ranging from T = 300 K to T = 3600 K. Those two properties can be determined from the temperature dependence of the exchange rate of the carbon atoms between two nanohorns and from the internal energy in the carbon atom aggregates. Two extreme nanohorn cases, i.e., $\theta = 30°$ and $\theta = 120°$, were studied. It is observed that the coalescence temperature (T_c) of the sharp nanohorn ($\theta = 30°$) is lower than that of the blunt nanohorn ($\theta = 120°$), i.e., 1400–1800 K compared to 1900–2200 K, respectively [29]. Nan et al. [30] have demonstrated that a majority of CNHs could resist the applied force over 900 μN, showing excellent load-bearing ability. They demonstrated that there is a similarity between the hydrostatic behavios of CNHs and single-walled nanotubes. They both present high structural stability under high pressure.

Unlike carbon nanotubes, the joint influence of the three-dimensionality of SWCNHs aggregate and the one-dimensionality of the individual moiety of SWNH aggregates, on the mechanical properties of polymers has been rarely explored. One example of using carbon nanohorns together with polymeric materials was presented by Fraczek-Szczypta and Blazewicz [31]. It does analyze a combination of polyacrylonitrile (PAN) matrix with carbon nanohorns; it was observed that the presence of SWCNHs in the PAN suspension affects the structure of nanocomposites after solidification, by changing the structural ordering of the polymer. Mechanical properties of single-walled carbon nanohorns (SWCNHs) and SWNCHs plus few-layer graphene (EG)-reinforced poly (vinyl

alcohol) (PVA) matrix composites have been studied by Kadambi et al. [32]. The hardness (*H)* and elastic modulus (E) of PVA were found to be improved by ~135% and ~315%, respectively, upon the addition of just 0.4 wt % SWCNHs. The dimensionality of carbon nanohorns, and their interaction with the polymer matrix are factors responsible for these improvements of the mechanical properties.

Oxidized carbon nanohorns and their nanocomposites were used as a sensing layer for different types of humidity sensors [33 - 42]. Recently, two types of nanocomposites oxidized single-wall carbon nanohorns (ox-SWCNHs - Fig. 1.) /polyvinylpyrrolidone (PVP - Fig. 2.) were synthesized, one using ox-SWCNHs/PVP at 1/1 (w/w) ratio and another with ox-SWCNHs/PVP in a 1/2 (w/w) ratio. Both nanocomposites were used as sensing layers in the design of a relative humidity resistive sensor. The sensor comprises an interdigitated (IDT) electrodes structure manufactured on a Si/SiO_2 wafer and the sensing layer which is deposited *via* the drop-casting method. The performances of the designed sensor are comparable to that of a commercially available capacitive relative humidity sensor, which is characterized by the fast response time, high sensitivity, and excellent stability in time [43]. However, no details about the mechanical and thermal properties of the sensing layers (and thus its stability in time) were included in the mentioned study. It is the purpose of this paper to initiate a preliminary study about the mechanical and thermal properties of an ox-SWCNHs/PVP composite, at the 1/1 (w/w) ratio.

2. Materials and Methods

The oxidized SWCNHs are purchased from Sigma Aldrich and are characterized by diameters in the 2 nm to 5 nm range and lengths between 40 nm and 50 nm. The PVP (purchased from Sigma Aldrich) has an average mol wt 40,000.

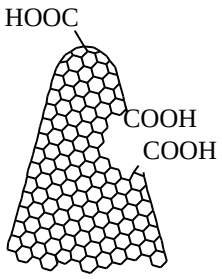

Fig. 1. The structure of oxidized carbon nanohorns

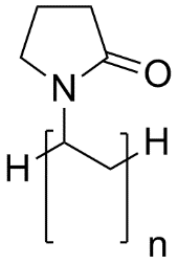

Fig. 2. The structure of PVP

2.1 Procedure of Sensor Preparation

First, it was established the design of the sensing IDT structure that is going to be fabricated on a Si wafer covered with 1 micron of SiO_2 (Fig. 3a. and

Fig. 3b.). The IDT's metal stripes were made by successive deposition of 10 nm chrome (Cr) and 100 nm gold (Au). The sensor has dimensions of 20 x 11 mm.

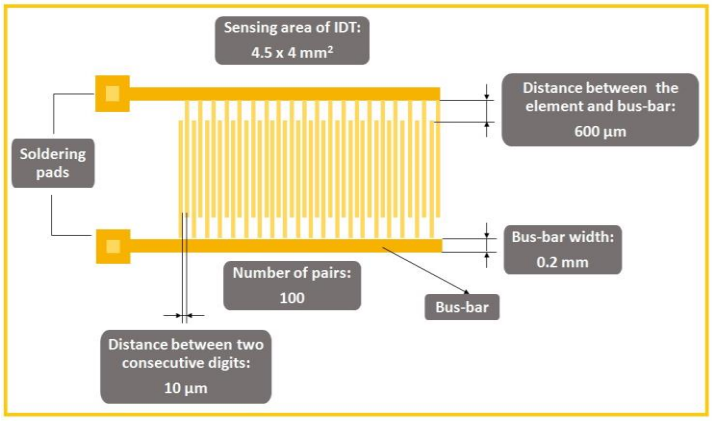

Fig. 3a. The structure of sensing IDT electrodes (100 pairs)

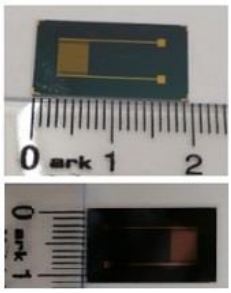

Fig. 3b. Dimensions of the chip

The solution is made of polyvinylpyrrolidone (PVP) and oxidized carbon nanohorns (1/1, w/w). 2 mg of Ox-SWCNHs were dispersed in 3 mL isopropyl alcohol and subjected to magnetic stirring (3500 rpm, for one hour at room temperature). Next, 2 mg of PVP was added in the first dispersion and were subjected again to magnetic stirring (2500 rpm, one hour at room temperature), followed by one hour of ultra-sonification. This ultrasonic homogenization part was implemented by using an Hielscher Ultrasonics UP200 St Equipment, with a working frequency of 26 kHz. The resulted dispersion of PVP / Ox-SWCNHs (1/1, w/w) solution was deposited in 8 successive layers by the "drop-casting" method on the IDT sensing structure. The layer thickness is measured with the Nova NanoSEM 630 (SEM) equipment from FEI Company.

After each deposition, we measured the electrical resistance with an Keithley 2700 Multimeter/Data Aquisition System equipment (Fig. 4.) from Keithley Instruments.

Fig. 4. Measuring the resistances

2.2 Characterization Techniques

2.2.1 Mechanical Stress

The mechanical tests were performed using a Mecmesin Multitest – i 2.5 equipment (Fig. 5.). This is a versatile, benchtop type tensile and compression tester (2 N up to 5 kN) controlled by software running on a PC.

Fig. 5. Mecmesin Multitest-i 2.5

Force testing is used to determine how a sample - subject to a tensile or compressive load (normal operation or when is being pulled or pushed) - reacts until it deliberately fails or breaks. When delivered suddenly at ultra-high speed, this is known broadly as 'dynamic' loading. It is typically used for cyclic-fatigue or creep testing to determine the life cycle of materials or components. However, it is much more common to measure the mechanical strength of an object by applying a load at a constant rate or varying it slowly (i. e.," static" or "monotonic" loading). Static force measurement is used as a quality-control method to comply with industry standards. It ensures the proper functioning of components and serves to record their safety and fitness for purpose. It can even help to determine the root cause of a wide variety of defects [44]. The testing was performed on the Si/SiO_2 structures with IDTs (20 x 11 mm) samples, differentiated by the number of layers obtained through "drop casting" 2 µL of the prepared solution and labeled as 1L, 2L, 3L, 4L, 5L, 6L, 7L and respectively 8L. Each sample went through a compressive load test, using the Mecmesin Multitest machine. The maximum load for the tests was set at 20 N, a value that was selected following the tests performed in which the maximum load until the sample breaks was 23 N (Fig. 6.). Young's modulus of elasticity (E) was determined using the equation:

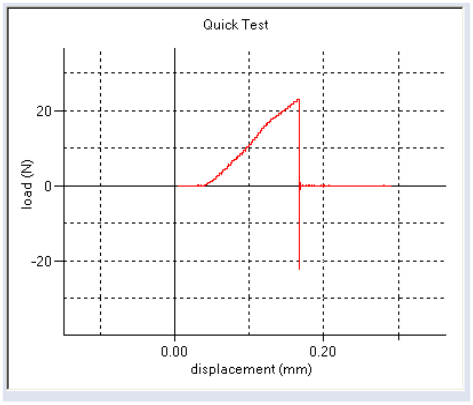

Fig. 6. The maximum load until the sample breaks

$$E \equiv \frac{\sigma(\varepsilon)}{\varepsilon} = \frac{F/A}{\Delta L/L_0} \quad (1)$$

where: **F** = the force exerted on an object under tension; **ΔL** = the amount by which the length of the object changes; $\mathbf{L_0}$ = the initial length of the object; **A** = the area of the device;

2.2.2. Temperature

One of the most challenging steps in the sensor's development is to verify how the environmental challenges affect their parameters, to be able to further compensate for these effects. In order to investigate the potential changes induced by the temperature, a Cryogenics 8200 Compressor (model CCS-450) was used for testing at temperatures below 50 ^oC. We used two samples (1 and 8 layers, respectively) for testing to see the reaction of the sensitive layer at different

environmental temperatures. In the first step the samples were exposed to mechanical stress, and the response was good, showing a high resistance. Before any experiments, the samples were observed through the optical microscope. Then the samples were tested at +50 ^{o}C and after that at -50 ^{o}C. When the tests ended, the samples were observed under the optical microscope in the same spot in order to see the changes.

3. Results and Discussion

By measuring the layer thickness with the Nova NanoSEM 630 equipment (Figures 7a – 7c), we can see that the thickness was approximately 200 nm. Of course, nanohorns agglomerations appear. The largest one measured was around 347.9 nm. The nanohorns arrange themselves next to each other, occupying the free spaces as the number of layers increases, to form a continuous layer.

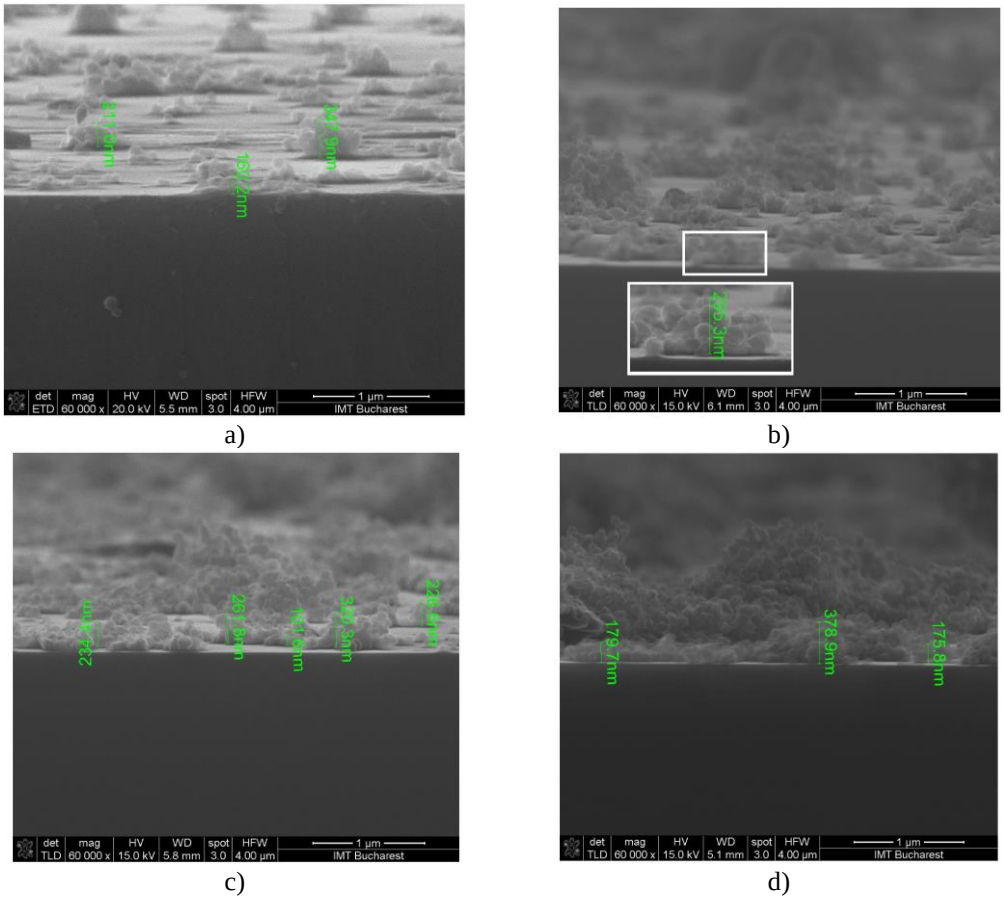

a) b)

c) d)

Fig. 7. SEM images of samples with: a) 1 layer; b) 4 layers; c) 8 layers; d) 20 layers

We wanted to see the reaction at 20 layers deposited on the substrate, and it seems that even more larger agglomerations appear (378.9 nm), but we can see

no interruptions of the layer, all the spaces were fulfilled (Fig. 7d.). After each deposition, we measured the electrical resistance, and the measured values are presented in Table 1. All the electrical resistances were measured at normal room temperature (23 ^{o}C, humidity 35%).

Table 1.

Values of electrical resistances for each sample

Number of Layer/s	1	2	3	4	5	6	7	8
Resistance [Ω]	838	827	814	798	742	705	640	562

Data from the typical responses (i.e., load force vs. displacement) from mechanical tests were collected and further analyzed (see Fig. 8a. for the sample with 1 layer and Fig. 8b. for the sample with 8 layers). First of all, it should be noted that the slope of the two characteristics changes during the measurements (at approx. 10 N for the 1L sample, and at approx. 8 N for the 8L sample). This means that they are no longer in linear mode. Young elasticity modulus (E) was calculated for the linear part for the sample with 1L and for the one with 8L. If we look at the data corresponding to a load force of 20 N, we can see that the values of the displacements are quite different between the two samples: 0.11 mm in one case (1L) and 0.20 mm for the sample with 8L.

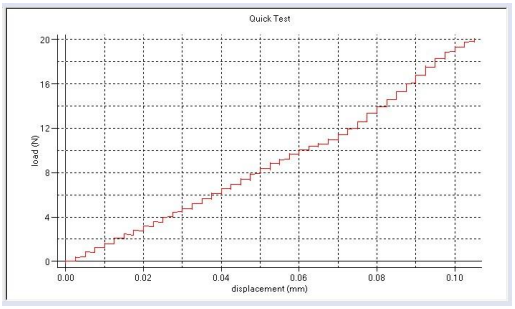

Fig. 8a. The variation of static load depending on deformation - Sample with 1 layer

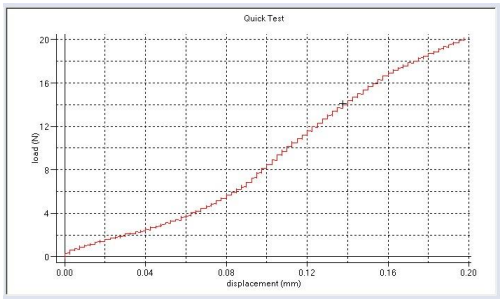

Fig. 8b. The variation of static load depending on deformation - Sample with 8 layers

The values of Young's modulus of elasticity for the samples with 1 layer and for the sample with 8 layers are presented in Table 2.

Table 2.

Values of Young's modulus of elasticity for the two samples

No. of layers	F (N)	ΔL (mm)	L_0 (mm)	A (mm^2)	**E (MPa)**
1 Layer (1L)	10	0.06	11	220	**8.33**
8 Layers (8L)	8	0.10	11	220	**3.99**

The solution used as sensitive layer consisting of oxSWCNHs and PVP on a Si/SiO_2 sensor with Au/Cr interdigitated electrodes has shown a 8.33 MPa elasticity when 1L sample is deposited on the sensitive area, and has an elasticity of 3.99 MPa for 8L deposited.

Studying the results obtained for all the samples, we can observe that the trend (i.e., the change in the E value, as the number of layers is increasing) is occurring in all samples, with a maximum change in E occurring for the sample consisting of 4 layers (see Fig. 9.). Fig. 9. does summarize the results from all the samples. We must also note that the increase of the elastic module is occurring at the same time with a decrease in the electrical resistance (for example, the dramatic decrease of the resistance between 7L to 8L).

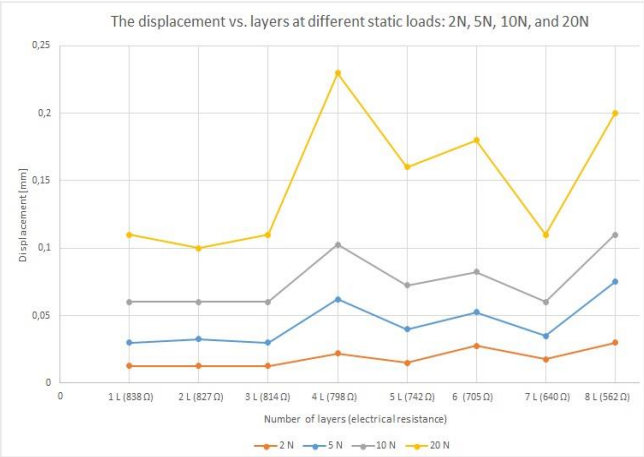

Fig. 9. The displacement graphic depending on the load

The results of temperature influence refer to two samples (1 and 8 layers, respectively) which were tested to see the reaction of the sensitive layer at different environmental temperatures. The optical microscopy images before and after the temperature experiments at +50 ^{0}C and -50 ^{0}C are presented in Fig. 10. A certain dynamics of cluster positioning can be observed, but no significant differences are recorded for the samples exposed at extreme temperatures of operation (+50 ^{o}C/-50 ^{o}C). From Fig. 10., we can see that the nanohorns can form agglomerations. We can also see that at -50 ^{o}C, the largest agglomeration was removed, but otherwise there cannot be seen any other important changes. So, from this point of view, the sensitive substrate responds very well to climatic changes.

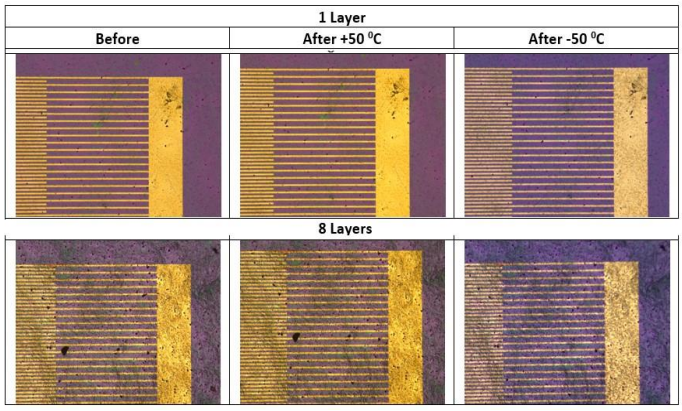

Fig. 10. Optical microscopy images for the samples with 1 layer and 8 layers

The resistance of the sensitive layer was also re-measured. As it was said before, at 8 layers deposited, the resistance was 562 Ω. After the tests at +50 ^{o}C, a resistance of 544 Ω was measured, and after the last treatment, at -50 ^{o}C the resistance was 611 Ω. A final 15 min furnace treatment at 110 ^{0}C was made, and after this the measured resistance was 534 Ω.

4. Conclusions

Nanocomposite layers based on ox-SWCNHs/PVP, which were proven as excellent relative humidity (RH) sensing layers [12], have been mechanically and thermally tested. The aim of the tests is twofold: a. to identify the correlation between their mechanical and electrical properties, thus allowing a future, optimized design of an RH sensor, on a rigid substrate; b. the asses their environmental stability. The results of the experiments performed indicated a change in the mechanical properties of the sensitive layers with the thickness (i.e., a decrease in Young's modulus). The elasticity value of the sensor with the sensitive layer that consists of 8 layers is, E = 3.99 MPa (reduced from 8.33 MPa for 1L). This behavior is accompanied by the changes in the electrical resistance of the layers, from 838 Ω to 562 Ω, a dramatic change being spotted at the transition from 7L to 8L. The functional properties of the layers were fully preserved after the thermal tests.

Acknowledgments

This work was funded by a grant of the Romanian Ministry of Research and Innovation, CCDI-UEFISCDI project number PN-III-P1-1.2-PCCDI-2017-0619/Nano-Carbon Plus. within PNCDI III and by the European Social Fund from the Sectoral Operational Programme Human Capital 2014-2020, through the Financial Agreement with the title "Scholarships for entrepreneurial education among doctoral students and postdoctoral researchers (Be Antreprenor!)", Contract no. 51680/09.07.2019 – SMIS code: 124539.

R E F E R E N C E S

[1]. *N. Jiang, J. E. Mück, and A. K. Yetisen*, "The regulation of wearable medical devices", in Trends in Biotechnology, **vol. 38**, no. 2, 2020, pp. 129-133.

[2]. *T. K. Gupta, P. R. Budarapu, S. R. Chappidi, S. Y. B. Sastry, M. Paggi, and S. P. A. Bordas*, "Advances in carbon-based nanomaterials for bio-medical applications," in Current Medicinal Chemistry, **vol. 26,** no. 38, 2019, pp 6851-6877.

[3]. *A. Raslan, L. Saenz del Burgo, J. Ciriza , J. L. Pedraz*, "Graphene oxide and reduced graphene oxide-based scaffolds in regenerative medicine," in International Journal of Pharmaceutics, **vol. 580**, 2020, 119226.

[4]. *P. Orsu, A. Koyyada*, "Recent progresses and challenges in graphene based nano materials for advanced therapeutical applications: a comprehensive review", in Materials Today Communications, **vol. 22,** 2020, 1000823.

[5]. *M. Dolatkhaha, N. Hashemzadeha, J. Barara, K. Adibkiaa, A. Aghanejada, M. Barzegar-Jalalib, Y. Omidia*, "Graphene-based multifunctional nanosystems for simultaneous detection and treatment of breast cancer", in Colloids and Surfaces B: Biointerfaces, **vol. 193,** 2020, 111104.

[6]. *N. Neuberger, H. Adidharma, M. Fan*, "Graphene: A review of applications in the petroleum industry", in Journal of Petroleum Science and Engineering, **vol. 167,** 2018, pp 152-159.

[7]. *C. A. Amadei, P. Arribas, C. D. Vecitis*, "Graphene oxide standardization and classification: Methods to support the leap from the lab to industry", in Carbon, **vol. 133** (2018), pp 398-409.

[8]. *L. Lancellotti, E. Bobeico, M. Della Noce, L. V. Mercaldo, I. Usatii, P. Delli Veneri , G. V. Bianco, A. Sacchetti, G. Bruno*, "Graphene as non conventional transparent conductive electrode in silicon heterojunction solar cells", in Applied Surface Science, **vol. 525,** 2020, 146443.

[9]. *L. Kaczmarek, T. Warga, P. Zawadzki, M. Makowicz, B. Bucholc, P. Kula*, "The influence of the hydrogenation degree on selected properties of graphene as a material for reversible H_2 storage", in International Journal of Hydrogen Energy, **vol. 44,** no. 41, 2019, pp 23149-23159.
[10]. *H. Song, Q. Li, Y. Zhang* "CNT-based sensor array for selective and steady detection of SO_2 and NO", in Materials Research Bulletin, **vol. 124,** 2020, 110772.
[11]. *M. V. Bracamonte, M. Melchionna, A. Giuliani, L. Nasi, C. Tavagnacco, M. Prato, P. Fornasiero;* "H_2O_2 sensing enhancement by mutual integration of single walled carbon nanohorns with metal oxide catalysts: The CeO_2 case", in Sensors and Actuators B: Chemical, **vol. 239,** 2017, pp 923-932.
[12]. *B. C. Serban, O. Buiu, N. Dumbravescu, C. Cobianu, V. Avramescu, M. Brezeanu, M. Bumbac, C. M. Nicolescu,* "Oxidized carbon nanohorns as novel sensing layer for resistive humidity sensor", in Acta Chimica Slovenica, **vol. 67,** no.2, 2020, pp 460-475.
[13]. *S. Li, Y. Ge, H. Li (Editors),* Smart Nanomaterials for Sensor Application, Bentham Science Publishers, 2012.
[14]. *D. Maiti, X. Tong, X. Mou and K. Yang,* "Carbon based nanomaterials for biomedical applications: A recent study, in Frontiers in Pharmacology, **vol.9**, 2019, DOI: 10.3389/fphar.2018.01401.
[15]. *M. Santos, M. M. M. Bilek, S. G. Wise,* "Plasma-synthesised carbon-based coatings for cardiovascular applications", in Biosurface and Biotribology, **vol. 1**, 2015, pp 146–160.
[16]. *T. Xie, L. Zhang, Y. Wang, Y. Wang, X. Wang,* "Graphene-based supercapacitors as flexible wearable sensor for monitoring pulse-beat", in Ceramics International, **vol. 45**, no. 2, Part A, 2019, pp 2516-2520.
[17]. *S. Reddy, X. Xu, T. Guo, R. Zhu, L. He, S. Ramakrishana,* "Allotropic carbon (graphene oxide and reduced graphene oxide) based biomaterials for neural regeneration", in Current Opinion in Biomedical Engineering**, vol. 6,** 2018, pp. 120-129**.**
[18]. *C. Redondo-Gómez, R. Leandro-Mora, D. Blanch-Bermúdez, C. Espinoza-Araya, D. Hidalgo-Barrantes and J. Vega-Baudrit,* "Recent advances in carbon nanotubes for nervous tissue regeneration", in Advances In Polymer Technology, **vol. 9**, 2020, Article ID 6861205;
[19]. *M. D. Angione, R. Pilolli, S. Cotrone, M. Magliulo, A. Mallardi, G. Palazzo, L. Sabbatini, D. Fine, A. Dodabalapur, N. Cioffi, L. Torsi,* "Carbon based materials for electronic bio-sensing", in Materials Today, **vol. 14**, no. 9, 2011, pp 424-433.
[20]. *S. A. Iyengar, P. Srikrishnarka, S. K. Jana, M. R. Islam ,T. Ahuja, J. S. Mohanty, and T. Pradeep,* "Surface-treated nanofibers as high current yielding breath humidity sensors for wearable electronics", in ACS Applied Electronic Materials, **vol. 1**, no. 6, 2019, pp 951-960.
[21]. *P. Salvo, F. Di Francesco, D. Costanzo, C. Ferrari, M. G. Trivella, D. De Rossi,* "A wearable sensor for measuring sweat rate", in IEEE Sensors Journal, **vol. 10**, no. 10, 2010, pp 1557-1558.
[22]. *M. M. Delgado-Povedanoa, M. Calderón-Santiagoa, M. D. Luque de Castroa, F. Priego-Capotea,* "Metabolomics analysis of human sweat collected after moderate exercise", in Talanta - The International Journal of Pure and Applied Analytical Chemistry, **vol. 177**, 2018, pp 47-65.
[23]. *C. Y. Cui, J. H. Noh, M. Michel, M. Gorospe, D. Schlessinger,* "STIM1, but not STIM2, is the calcium sensor critical for sweat secretion", in Journal of Investigative Dermatology, **vol. 138,** no. 3, 2017, pp 704-707.
[24]. *S. Robinson, A. H. Robinson,* "Chemical Composition of Sweat", in Physiological Reviews, **vol. 34,** no. 2, pp 202-220, 1954.
[25]. *S. Iijima, M. Yudasaka, R. Yamada, S. Bandow, K. Suenaga, F. Kokai, K. Takahashi*, "Nano-aggregates of single-walled graphitic carbon nano-horns", in Chemical Physics Letters, **vol. 309,** no. 3-4, 1999, pp 165 - 170.
[26]. *B. C. Serban, M. Bumbac, O. Buiu, C. Cobianu, M. Brezeanu, C. M. Nicolescu,* "Carbon nanohorns and their nanocomposites: Synthesis, properties, and applications. A concise review", in Annals of the Academy of Romanian Scientists Series on Science and Technology of Information, **vol. 11,** no. 2, 2018, pp 5-18.
[27]. *J. Miyawaki, R. Yuge, T. Kawai, M. Yudasaka, S. Iijima*, "Evidence of thermal closing of atomic-vacancy holes in single-wall carbon nanohorns", in Journal of Physical Chemistry C **vol. 111,** 2007, pp. 1553–1555.

[28]. *J. Fan, R. Yuge, J. Miyawaki, T. Kawai, S. Iijima, M. Yudasaka*, "Close-open-close evolution of holes at the tips of conical graphenes of single-wall carbon nanohorns", in Journal of Physical Chemistry C, **vol. 112,** no. 23, 2008, pp 8600–8603.

[29]. *P. C. Tsai, Y. R. Jeng*, "Theoretical investigation of thermally induced coalescence mechanism of single-wall carbon nanohorns and their mechanical properties", in Computational Materials Science, **vol. 88**, 2014, pp 76-80.

[30]. *Y. Nan, B. Li , X. Zhao, X. Song, L. Su*, "Probing the mechanical properties of carbon nanohorns subjected to uniaxial compression and hydrostatic pressure", in Carbon, **vol. 125,** 2017, pp. 236-244.

[31]. *A. Fraczek-Szczypta, S. Blazewicz, „*Manufacturing and physico-mechanical characterization of carbon nanohorns/polyacrylonitrile nanocomposites", in Journal of Materials Science, **vol. 46**, 2011, pp 5680-5689.

[32]. *S. B. Kadambi, K. Pramoda, U. Ramamurty, C. N. R. Rao*, "Carbon-nanohorn-reinforced polymer matrix composites: synergetic benefits in mechanical properties", in ACS Applied Materials & Interfaces, **vol. 7**, no. 31, 2015, pp 17016-17022.

[33]. *B. C. Șerban, O. Buiu, C. Cobianu, V. Avramescu, N. Dumbrăvescu, M. Brezeanu, M. Bumbac, C. M. Nicolescu and R. Marinescu,* „Ternary Carbon-Based Nanocomposite as Sensing Layer for Resistive Humidity Sensor", in Multidisciplinary Digital Publishing Institute Proceedings, **vol. 29**, no. 1, 2019, pp 114.

[34]. *B. Serban, O. Buiu, C. Cobianu, R. Marinescu, V. Avramescu, N. Dumbravescu,* Switch-type chemiresistive humidity sensor, Romanian application patent, OSIM, A/00442/22.07.2019

[35]. *B. Serban, O. Buiu, C. Cobianu, V. Avramescu, N. Dumbravescu, R. Marinescu,* Chemiresistive humidity sensor based on oxidized carbon nanohorns, Romanian application patent, OSIM,A/00443/22.07.2019.

[36]. *B. Șerban, O. Buiu, C. Cobianu, V. Avramescu, N. Dumbrăvescu, R. Marinescu,* Resistive sensor for relative humidity monitoring and method of making it, Romanian application patent, OSIM A/00517/28.08.2019;

[37]. *B. Șerban, O. Buiu, C. Cobianu, V. Avramescu, N. Dumbrăvescu, R. Marinescu,* Matrix nanocompozite for SAW humidity sensor, Romanian application patent A/005;18/28.08.2019;

[38]. *B. Șerban, O. Buiu, C. Cobianu, V. Avramescu, N. Dumbrăvescu, R. Marinescu,* Polyelectrolyte-oxidized carbon nanohorn based on matrix nanocompozite for resistive humidity sensor and method of making it, Romanian application patent A/00521/28.08.2019

[39]. *B. C. Serban, C. Cobianu, N. Dumbravescu, O. Buiu, M. Bumbac, C. M. Nicolescu*, "Oxidized carbon nanohorns as novel sensing layer for chemiresistive humidity sensor", S-1 P-20, 9th International Conference of the Chemical Societies of the South-Eastern European Countries on "Chemistry a nature challenger", May 8th – 11th, 2019, Târgoviște, România.

[40]. *B. C. Serban, C. Cobianu, N. Dumbravescu, O. Buiu, C. M. Nicolescu, M. Bumbac*, "Hydrophilic polymer - oxidized carbon nanohorns compozite - based chemiresistive humidity sensor", S5_P_15, 9th International Conference of the Chemical Societies of the South-Eastern European Countries on "Chemistry a nature challenger", May 8th – 11th, 2019, Târgoviște, România

[41]. *R. Marinescu, B. Serban, N. Dumbravescu, V. Avramescu, C. Cobianu, O. Buiu*, "Carbon-based materials for healthcare micro-devices", in Nonconventional Technologies Review, **vol**. **23,** no. 4, 2019, pp 72-77.

[42]. *B. C. Serban, O. Buiu, C. Cobianu, V. Avramescu, I. C. Pachiu, N. O. Ionescu, R. Marinescu,* Chemiresistive humidity sensor based on matrix nanocomposites containing hydrophilic carbon nanohorns, OSIM Patent Application No. A/ 01006 din data de 29- 11- 2018.

[43]. *B. C. Serban, O. Buiu, N. Dumbravescu, C. Cobianu, V. Avramescu, M. Brezeanu, M. Bumbac, C. M. Nicolescu*, "Oxidized carbon nanohorn-hydrophilic polymer nanocomposite as the resistive sensing layer for relative humidity", in Analytical Letters, published on-line 12 June 2020, DOI: 10.1080/00032719.2020.1772805, pp 1-14.

[44]. www.mecmesin.com , accesed at 23.10.2019.